Korean J. Chem. Eng., **27**(3), 766-776 (2010)
DOI: 10.1007/s11814-010-0119-5

Mathematical modeling of CO_2 removal using carbonation with CaO: The grain model

Behnam Khoshandam*,†, Ramachandran Vasant Kumar, and Leila Allahgholi***

*Chemical Engineering Department, Semnan University, Semnan, Iran
**Department of Materials Science and Metallurgy, University of Cambridge, Cambridge, UK
(*Received 3 June 2009 • accepted 15 September 2009*)

Abstract−CaO carbonation with CO_2 is potentially a very important reaction for CO_2 removal from exhaust gas produced in power plants and other metallurgical plants and for hydrogen production by promoting water gas shift reaction in fossil fuel gasification. A mathematical model based on the grain model was applied for modeling of this reaction. Diffusion of gaseous phase through the product layer and structural change of the grains were considered in the model. The modeling results show that ignoring the reaction kinetics controlling regime in the early stage of the reaction and replacing it with a regime considering both the reaction kinetics and diffusion can generate good simulation results. The frequency factor of the reaction rate equation and the diffusivity of CO_2 through the $CaCO_3$ layer were justified to get the best fit at different temperature range from 400 to 750 °C with respect to experimental data in the literature. The mathematical model switches to a pure diffusion controlling regime at final stage of reaction.

Key words: CaO Carbonation, CO_2 Removal, Mathematical Modeling, Porous Media, Diffusion

INTRODUCTION

Current levels of CO_2 concentration at 380 ppm have increased by 100 ppm since the year 1800, starting at the early stages of the industrial revolution [1]. Human activities are responsible for emitting 22 billion tons of CO_2 gas each year mainly from fossil fuel combustion. As the main greenhouse gas, it is the most important player contributing over 60% to the global greenhouse effect in the climate change stake. Removing CO_2 from industrial processes using different methods is one of the major problems in this and the subsequent decades.

CO_2 sequestration consists of capture and storage of CO_2. The main CO_2 capture technologies are based on absorption (chemical and physical), cryogenics and membrane technologies [2]. A good discussion of these methods and comparisons was reported by Eloneva [1]. The main methods to store captured CO_2 are ocean sequestration, deep underground storage and storage as an inert solid by mineral carbonation reaction.

CaO carbonation is based on the reaction of CaO with CO_2 to yield a layer of porous $CaCO_3$ around CaO. A study of the carbonation reaction was carried out by Bhatia and Perlmutter [3]. They considered the formation of nucleation sites of $CaCO_3$ as a rate controlling step. They reported values of 87.9 kJ mol^{-1} and 179.9 kJ mol^{-1} for activation energies at temperatures below and above 415 °C, respectively, for reaction rate control by diffusion through the product-layer. Dedman, Owen [4] and Okeson & Culter [5] reported a two-step mechanism for the reaction rate - chemical reaction control at lower conversion levels and diffusion control at higher conversion levels. The total CaO conversion in carbonation reaction was reported in the range of 70-90% [3,6,7]. The difficulty in achieving total conversion has been ascribed to the unfavorable initial pore size distribution in the CaO sorbent [8].

The carbonation reaction of CaO with CO_2 can be represented by:

$$CaO(solid)+CO_2(gas)\rightarrow CaCO_3(solid) \quad (1)$$

The kinetic data for this reaction has shown that initially the rate is rapid and chemically controlled, but then undergoes a sudden transition to a slower diffusion controlled regime [6,8,9]. Based on the nature of the reaction, it seems that a pure chemical reaction controlling regime is very short in duration and can be neglected without much error in the mathematical modeling. Therefore, the modeling can commence with a regime of simultaneous chemical and diffusion controlling step then followed by a pure diffusion controlling regime.

Three different models based on the random pore model, the shrinkage unreacted core model and the grain model are reported for carbonation reaction of CaO with CO_2. They describe structural changes of solid reactant during the reaction [10]. The grain model is a general model that has been used by many researchers to study non-catalytic gas-solid reactions. In this model, the solid pellet is considered as made up of a number of grains, which are surrounded by pores through which the gas can diffuse to reach the various grains. This model can cover different situations arising from shrinking core model (SCM) in non-porous pellets to volume model (VM) in highly porous pellets. In the present work, the grain model has been developed by considering different controlling stages of reaction rate for the carbonation reaction.

The modeling is carried out on a single pellet reacting under two different regimes - simultaneous chemical reaction and diffusion control in the first stage, followed by a diffusion controlling step alone. The parameters of mathematical model were justified in the two steps to achieve the best fit with respect to experimental data

†To whom correspondence should be addressed.
E-mail: bkhoshandam@semnan.ac.ir

and sensitivity analysis was carried out for the model.

CARBONATION REACTION OF CaO

At the very early stage of the reaction, a heterogeneous reaction occurs rapidly and the rate of reaction is controlled by chemical reaction. Following the initial stage, the solid product layer is formed on the outer surface of a CaO particle and the rate of reaction is controlled by diffusion of gaseous reactant thorough the solid product and this rate decreases with time.

CaO sorbents from natural sources normally fail to achieve complete conversion due to nano-porous structure (<2 nm), while mesoporous CaO sorbents (5-20 nm) obtained by chemical methods are reported to achieve high degree of conversions at over 90% [6].

Nano-porous sorbents (pore size <2 nm) are susceptible to pore blockage through the formation of high-molar volume product layer (molar volume of $CaCO_3$=37 cm^3 mol^{-1}; molar volume of CaO= 16 cm^3 mol^{-1}). Mesoporous sorbents (pore size 5-20 nm) are less susceptible to pore blockage [6].

The activation energy in the carbonation of surface CaO with CO_2 is estimated to about 72 kJ mol^{-1} regardless of the source of CaO in the diffusion controlling regime and is about 102 kJ mol^{-1} in reaction controlling regime for mesoporous CaO [8,9] or 189 kJ mol^{-1} for commercially available CaO [3,8], most probably relating to morphological differences between the various CaO samples.

For chemical reaction control at the interface the CaO micro- and nano-structure is not expected to be critical, but after passing through this stage, the reaction kinetic plays decreasing role in progress of the reaction and the diffusion phenomenon has the major role in determining the rate. Therefore, in the following sections, the reaction of a porous CaO pellet that is immersed in a stream of pure CO_2 is modeled using the grain model.

MATHEMATICAL MODELING

In practice, the reacting gas CO_2 will diffuse from the bulk of a gas to the porous pellet surface through a boundary layer around the pellet and then diffuses into the pellet. During the diffusion of CO_2 into the pellet, a carbonation reaction occurs with the grains.

Fig. 1 shows a schematic representation of the reaction. The outer circle is the pellet and the smaller circles inside represent the grains and the black zone inside grains is unreacted CaO core. The CO_2 is considered to diffuse through a product layer produced around the grains to reach the solid reactant CaO. The grains near center of the pellet can be expected to have more unreacted CaO zones because of the diffusion process of gaseous reactant CO_2 inside the pellet.

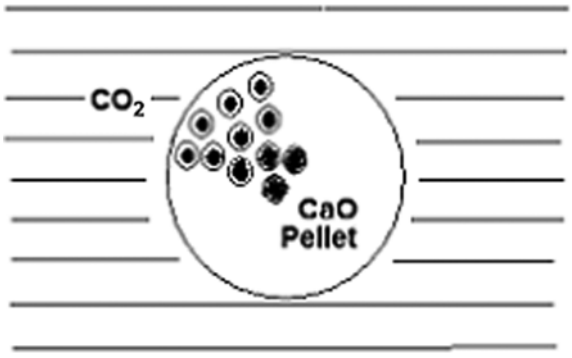

Fig. 1. A porous CaO pellet containing a large number of grains reacting with CO_2 (the unreacted core inside the grains is shown by the black region).

1. Assumptions

The following assumptions are made in the development of the mathematical model:

1. The reaction is irreversible.
2. The pressure is constant.
3. The regime corresponds to an unsteady state for gaseous concentration inside the pellet.
4. Although the reaction is exothermic, because of low rate of conversion, isothermal condition is considered to prevail. Thus, the temperature gradient is neglected in both the overall pellet and within the individual grains.
5. Reaction is defined as a first-order reaction.
6. Three different geometrical shapes - flat plate, cylindrical and spherical - are considered for the porous pellet.
7. The pellet is made from grains of different geometries by compression.
8. The individual grains are considered to be non-porous.
9. The resistance of diffusion in the boundary layer outside the pellet from bulk of the gas flow to the surface of pellet is considered.
10. The grain dimensions can vary with time due to the differences in the molar volume of the solid reactant and the solid product.
11. The porosity variation in the pellet is considered dependent upon the grain size and the volume of the grain.
12. Diffusion of reactant gas through the product layer around the grains is considered.
13. Effective diffusivity of gas inside the pellet is considered to vary as square of the porosity.

2. Governing Equations

The mass balance equation for the gaseous reactant, CO_2, in the pellet made of CaO grains with different geometries is written as:

$$\frac{\partial(\varepsilon C_{CO2})}{\partial t} = \frac{1}{z^{F_p-1}}\frac{\partial}{\partial z}\left(z^{F_p-1} D_e \frac{\partial C_{CO2}}{\partial z}\right) + F_g(1-\varepsilon_0)\frac{r_c^{F_g-1}}{r_0^{F_g}} f_G \tag{2}$$

where C_{CO2} is the CO_2 concentration, ε is the pellet porosity as a function of grain radius, t and z are independent variables of time and the radial coordinate in the pellet, respectively, D_e is the effective diffusivity of CO_2 inside the pellet as a function of porosity, ε_0 is the initial pellet porosity, r_c and r_0 are the radial position of the reaction front inside the pellet and initial radius of the grains, respectively, f_G is the surface reaction rate and F_p and F_g are pellet and grain shape factors, respectively (=1, 2 and 3 for flat, cylindrical and spherical shapes, respectively). The initial and boundary conditions for this equation are written as follows:

$$C_{CO2}(t=0) = C_{CO2,0} \tag{3}$$

$$\left.\frac{\partial C_{CO2}}{\partial z}\right|_{z=0} = 0 \tag{4}$$

$$D_e \left.\frac{\partial C_{CO2}}{\partial z}\right|_{z=r_p} = k_c(C_{CO2,b} - C_{CO2,s}) \tag{5}$$

where subscripts 0, b and s indicate the initial value, the value in

the bulk and on the pellet surface, respectively, r_p is the pellet radius and k_c is the convective mass transfer coefficient.

The mass balance equation for the CaO grains is simply written as an equation for radial position of reaction front inside grains, r_c, as follows.

$$\frac{dr_c}{dt} = \frac{M_{CaO}}{\rho_{CaO}} f_G \tag{6}$$

where M and ρ denote the molecular weight and density, respectively. The initial condition for this equation is written as:

$$r_c(t=0)=r_0 \tag{7}$$

Modeling should cover two stages. The first stage covers the reaction kinetics and diffusion control simultaneously and second stage corresponds to only diffusion control through the product layer.

2-1. Stage 1: Reaction Kinetics and Diffusion Control Simultaneously

The mass balance equation for the gaseous reactant through the product layer around grains (in flat, cylindrical or spherical geometry) is derived as follows, respectively for the three shapes [11]:

$$C_{CO2,i} = \frac{f_G}{D_{CO2,p}}(r_c - r_g) + C_{CO2} \tag{8}$$

$$C_{CO2,i} = \frac{r_c f_G}{D_{CO2,p}} \ln(r_c/r_g) + C_{CO2} \tag{9}$$

$$C_{CO2,i} = \frac{r_c f_G}{D_{CO2,p}} \frac{(r_c - r_g)}{r_g} + C_{CO2} \tag{10}$$

where $C_{CO2,i}$ is the CO_2 concentration at the interface between the product layer and the reactant CaO, $D_{CO2,p}$ is the diffusion coefficient of CO_2 through the product layer and r_g is the grain radius as a function of reaction front radial position, r_c, (described in the next section). It can be noted that the surface reaction rate, f_G, is a function of $C_{CO2,i}$ and therefore the Eqs. (8)-(10) can be rearranged and simplified. For example, for the spherical grains with a first-order reaction kinetics with respect to the gaseous reactant CO_2 (substituting $kC_{CO2,i}$ for f_G), Eq. (10) can be rearranged as:

$$C_{CO2,i} = \frac{C_{CO2}}{\left(1 - \frac{r_c k (r_c - r_g)}{D_{CO2,p} r_g}\right)} \tag{11}$$

where k, in this equation is reaction rate constant and is a function of temperature.

2-2. Stage 2: Diffusion Control

When CO_2 diffusion through the product layer around grains is controlling the reaction rate, Eqs. (8)-(11) cannot be used to model the reaction. In this stage, the diffusion coefficient through the product layer should tend towards zero with time. Porosity and tortuosity variations are the main reasons for the decreasing value of diffusion coefficient. In this section an approximate mathematical relationship is initially considered. In the next section, the relationship between porosity and grain radius is incorporated in order to improve the representation of reality within the model.

Therefore, in this stage, Eq. (11) is replaced by a mathematical relation showing decreasing value of CO_2 concentration at the reaction front. As noted by Levenspiel [12], under diffusion control, the gaseous reactant concentration at the interface between the product layer and the solid reactant unreacted core should be zero. The following Eq. (12) was found to show a good agreement with experimental data:

$$C_{CO2,i} = \frac{A}{t^n} + B \tag{12}$$

where A, B and n are constants. The following conditions can be incorporated by the above equation:

$$\text{at } t=t_{f,1},\ C_{CO2,i}=C_{CO2,i,f} \tag{13}$$

$$\text{as } t\to\infty,\ C_{CO2,i}=0 \tag{14}$$

where $t_{f,1}$ and $C_{CO2,i,f}$ are the final time and CO_2 concentration at the reaction front achieved during the first stage. After replacing the conditions above in Eq. (12), B=0, $A=C_{CO2,i,f}\, t_{f,1}^n$ and the following equation is obtained:

$$C_{CO2,i} = \left(\frac{t_{f,1}}{t}\right)^n C_{CO2,i,f} \tag{15}$$

A good fit to experimental data at the second stage was achieved when a value of 1.7 for n was assigned.

3. Auxiliary Equations

The following auxiliary equations have to be considered in the modeling. The first-order surface reaction rate can be defined as follows.

$$f_G = kC_{CO2,i} \tag{16}$$

where k is the reaction rate coefficient as a function of temperature as determined by the Arrhenius equation:

$$k = k' e^{-\frac{E_a}{RT}} \tag{17}$$

where k' is a constant, the frequency factor, E_a is the activation energy of reaction, R is the gas constant and T is the temperature.

Variation in grain radius can be approximated from the mass balance equation for the solid reactant CaO as follows:

$$r_g = \left(\frac{(r_0^{F_g} - r_c^{F_g})\rho_{CaO} M_{CaCO3}}{1-\varepsilon_{CaCO3}\rho_{CaCO3} M_{CaO}} + r_c^{F_g}\right)^{1/F_g} \tag{18}$$

where ε_{CaCO3} is the porosity of $CaCO_3$.

The porosity of CaO can vary as a function of grain radius as follows [13]:

$$\varepsilon = 1 - (1-\varepsilon_0)\left(\frac{r_g}{r_0}\right)^{F_g} \tag{19}$$

In this equation it is assumed that the overall volume of the pellet is not changing during the course of the reaction.

The effective diffusion coefficient can vary as a function of porosity based on the random pore model of Wakao and Smith [14] as follows:

$$D_e = D_{e0}\left(\frac{\varepsilon}{\varepsilon_0}\right)^2 \tag{20}$$

where the subscript 0 shows the initial value of the parameter.

The conversion of the grains in different geometries is defined as follows [13].

$$x = 1 - \left(\frac{r_c}{r_0}\right)^{F_g} \tag{21}$$

The integration of conversions x inside the pellet makes the overall

conversion X of the pellet as follows:

$$X = \frac{\int_0^{r_p} z^{F_p-1} x dz}{\int_0^{r_p} z^{F_p-1} dz} \quad (22)$$

The effective diffusivity is obtained with the aid of the Bosanquet interpolation formula [15]:

$$D_e = \left(\frac{\varepsilon}{\tau}\right)\left(\frac{1}{D_M} + \frac{1}{D_K}\right)^{-1} \quad (23)$$

where τ is tortuosity of the pellet, which is defined as reciprocal of porosity. Also D_M and D_K are molecular and Knudsen diffusivity of

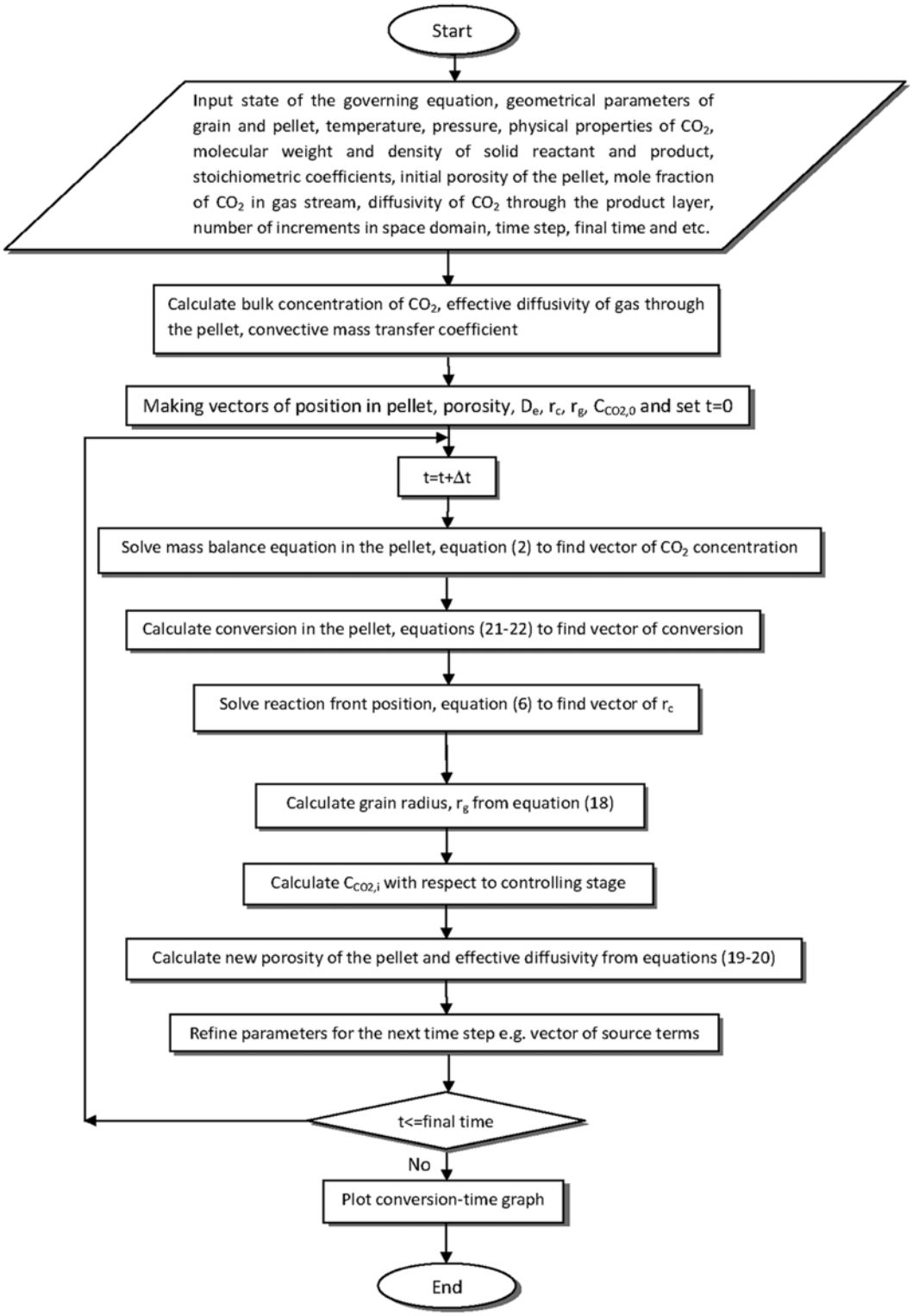

Fig. 2. Algorithm of the solution method.

CO_2 inside the pellet, respectively. The Knudsen diffusivity can be calculated from [13]:

$$D_k = \frac{4}{3}\left(\frac{8RT}{\pi M_{CO2}}\right)^{1/2} k_0 \tag{24}$$

where k_0 is a factor determined by the void fraction, the pore size distribution and the pore geometry that from "dusty gas model" of Mason et al. [16] for a solid matrix made of uniform spherical grains the following equation is proposed.

$$k_0^{-1} = \left(\frac{128}{9}\right) n_d r_g^2 \left(1 + \frac{\pi}{8}\right) \tag{25}$$

Finally, the number of solid grains per unit volume of porous solid, n_d, is calculated from a simple mathematical relation as a function of porosity and the grain radius as:

$$n_d = \frac{3(1-\varepsilon)}{4\pi r_g^3} \tag{26}$$

Increasing number of grains per unit volume of porous solid results in effective diffusivity to decrease from reducing the k_0 value as calculated in Eq. (25).

SOLUTION METHOD

The finite volume integration of partial differential Eq. (2), over a control volume (CV) with a further integration over a finite time step is applied for the discretization process of this equation [11].

$$\int_z^{z+\Delta z}\left(\int_t^{t+\Delta t}\frac{\partial(\varepsilon C_{CO2})}{\partial t}dt\right)z^2dz = \int_t^{t+\Delta t}\left(\int_z^{z+\Delta z}\frac{\partial}{\partial z}\left(z^2 D_e\frac{\partial C_{CO2}}{\partial z}\right)dz\right)dt + \int_t^{t+\Delta t}\left(\int_z^{z+\Delta z} 3(1-\varepsilon_0)\frac{r_c^2}{r_0^3}kC_{CO2}z^2dz\right)dt \tag{27}$$

The accumulation term has been discretized by using a first-order backward differencing scheme. Indeed, for the diffusion term, we apply central differencing.

After the discretization process, a system of algebraic equations is solved at each time level implicitly. The time marching procedure starts with a given initial field of concentration as given by Eq. (3). For each time level, all dependent parameters are also renewed. Next, the solution C_{CO2} are assigned to $C_{CO2,0}$ and the procedure is repeated to progress the solution by a further time step.

PROGRAM FLOWCHART

A computer program developed in MATLAB was used to solve equations. The algorithm of solution is presented in Fig. 2.

RESULTS AND DISCUSSION

Two sets of experimental data were used to compare with mathematical modeling results. The first set was taken from Bhatia and Perlmutter [3]. They carried out experiments with synthetic CaO samples with varying grain sizes which were reacted with carbon dioxide at different temperatures. The second set of experimental data was obtained by Lee et al. [7]. The rate of conversion is higher in the first data set in comparison with the second set. The modeling of different data is described in the following sections.

1. Experimental Data of Bhatia and Perlmutter [3]

The experiments of Bhatia and Perlmutter [3] were carried out in the temperature range of 400 to 725 °C with CO_2 mole fractions varying from 0.1 to 0.42 in a mixture with nitrogen. The CaO samples used in their experiments made from decomposing the limestone in a thermogravimetric analyzer. The resulting CaO had different pore structures. In these experiments it was assumed that the CO_2 diffuses through the pellets (51% porosity) prepared from nonporous CaO grains and that there is no CO_2 concentration gradient in the pellet. The parameters used in our mathematical modeling are presented in Table 1 for CO_2 mole fraction of 0.1 reacted with

Table 1. Parameters used in modeling of experimental data of Bhatia and Perlmutter [3] at low temperatures and CO_2 mole fraction

Activation energy (kJ mol^{-1})	72
Grain radius (nm)	10
Initial porosity	0.51
CO_2 mole fraction	0.1
pressure (atm)	1
Density of CaO (kg m^{-3})	3320
Porosity of $CaCO_3$	0.4- 0.35- 0.29
Density of $CaCO_3$ (kg m^{-3})	2800
Temperature (°C)	400- 438- 480

Table 2. Justifying parameters in the mathematical modeling of data of Bhatia and Perlmutter [3] at low temperatures and CO_2 mole fraction

Justifying parameter	Value
k' (m s^{-1})	1.7
$D_{CO2,p}$ at 400 °C (m^2 s^{-1})	1.4e-13
$D_{CO2,p}$ at 438 °C (m^2 s^{-1})	3.6e-13
$D_{CO2,p}$ at 480 °C (m^2 s^{-1})	8e-13

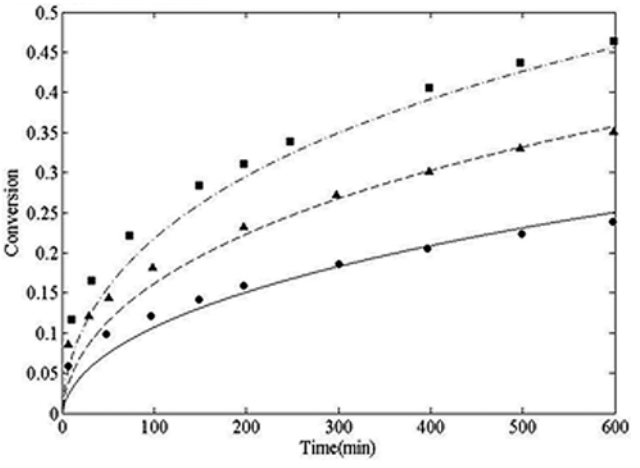

Fig. 3. A comparison between simulation results and experimental data of Bhatia and Perlmutter [3] at low temperatures, squares (480 °C, 753 K), triangles (438 °C, 711 K), circles (400 °C, 673 K).

CaO at different temperatures of 400, 438 and 480 °C. The justifying parameters in program are shown in Table 2 for three sets of data at three different temperatures. Fig. 3 shows a comparison between simulation results and experimental data in this case. As it can be seen the agreement of simulation results with experimental data is not good at this first stage, but it should be expected to get better with time. Neglecting the early duration stage pertaining to pure reaction kinetics, the controlling step may be responsible for generating these errors; but after this short stage the reaction continues in the next stage pertaining to simultaneous reaction kinetics and diffusion controlling step and a good agreement can be noted. As it seen in this figure, the reaction continues in this stage and the last stage of diffusion control cannot have occurred as yet.

Table 3. Parameters used in modeling of experimental data of Bhatia and Perlmutter [3] at high temperatures and CO_2 mole fraction

Activation energy (kJ mol^{-1})	72
Grain radius (nm)	10
Initial porosity	0.51
CO_2 mole fraction	0.42
pressure (atm)	1
Density of CaO (kg m^{-3})	3320
Porosity of $CaCO_3$	0.2- 0.15- 0.13
Density of $CaCO_3$ (kg m^{-3})	2800
Temperature (°C)	585- 615- 655

Table 4. Justifying parameters in the mathematical modeling of data of Bhatia and Perlmutter [3] at high temperatures and CO_2 mole fraction

Justifying parameter	Value
k′ (m s^{-1})	1.7
$D_{CO2,p}$ at 585 °C (m^2 s^{-1})	4.7e-12
$D_{CO2,p}$ at 615 °C (m^2 s^{-1})	1.4e-11
$D_{CO2,p}$ at 655 °C (m^2 s^{-1})	3e-11

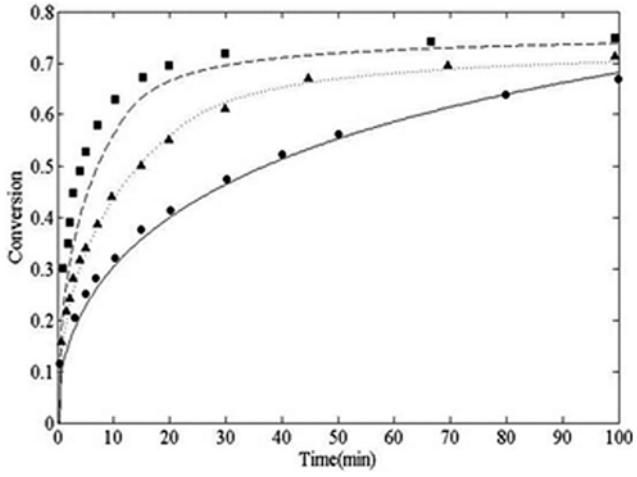

Fig. 4. A comparison between simulation results and experimental data of Bhatia and Perlmutter [3] at high temperatures, squares (655 °C, 928 K), triangles (615 °C, 888 K), circles (585 °C, 858 K).

The mathematical modeling was carried out on three other sets of data at higher temperatures. In this case the carbonation reaction was done at a CO_2 mole fraction of 0.42 at temperatures of 585, 615 and 655 °C. The data used in program with the grain model is presented in Table 3. After justifying the frequency factor of reaction constant and diffusion coefficient of CO_2 through product layer around grains as depicted in Table 4, the conversion-time graphs are drawn as Fig. 4. As can be seen the agreement is good at 585 °C and the differences between simulation results and experimental data become more divergent as temperature increases. The agreement in early times of reaction is not good because of the aforementioned reason. What is important in this figure is that the reaction at 585 °C is not accompanied by pure diffusion controlling regime unlike those of reactions at 615 and 655 °C. The reactions at these two higher temperatures show a decline in conversion rate with time as a result of reaction entering the last stage of pure diffusion control after duration of 10 min.

As shown in Table 2 and Table 4, the diffusion coefficients are functions of temperature. The activation energy in the simultaneous reaction kinetics and diffusion controlling step can be calculated from Bhatia and Perlmutter data as 93 kJ mol^{-1}. Also, in the last stages pertaining to pure diffusion control, the activation energy is calculated as 173 kJ mol^{-1}. The reported values of the activation energies are 88.9±3.7 and 179.2±7.0 kJ mol^{-1} in the random pore model by Bhatia and Perlmutter [3]. The simulation results in the present work show good agreement with the experimental results.

2. Experimental Data of Lee et al. [7]

In the work presented by Lee et al. [7], the carbonation reaction of spherical pellets prepared from CaO grains with pure stream of CO_2 was carried out in a thermogravimetric analyzer at different temperatures in the range between 650 and 700 °C. The parameters needed in mathematical modeling of carbonation reaction based

Table 5. Parameters used in modeling of experimental data of Lee et al. [7]

Diameter of the pellet (m)	0.003
Grain radius (nm)	7
Initial porosity	0.45
CO_2 mole fraction	1
pressure (atm)	1
Activation energy (kJ mol^{-1})	72
Density of CaO (kg m^{-3})	3320
Porosity of $CaCO_3$	0.2
Density of $CaCO_3$(kg m^{-3})	2800
Temperature (°C)	650-700-750

Table 6. Justifying parameters in the mathematical modeling of data of Lee et al. [7]

Justifying parameter	Value
k′ (m s^{-1})	0.012
$D_{CO2,p}$ at 650 °C (m^2 s^{-1})	6e-14
$D_{CO2,p}$ at 700 °C (m^2 s^{-1})	2e-13
$D_{CO2,p}$ at 750 °C (m^2 s^{-1})	8e-13

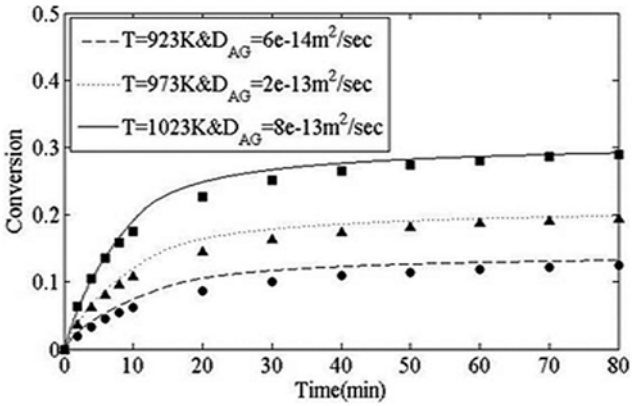

Fig. 5. A comparison between the experimental data (markers) of Lee et al. [7] and simulation results (lines) at different temperatures.

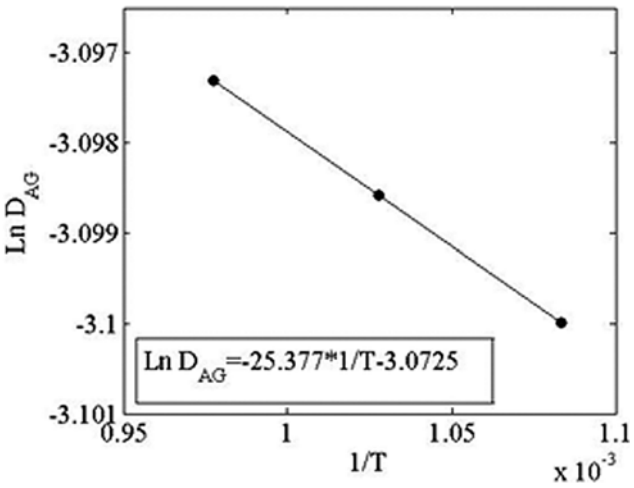

Fig. 6. Arrhenius plot to obtain activation energy in the kinetics and diffusion controlling stage.

on the Lee et al. [7], are presented in Table 5. Also, the parameters that were justified are depicted in Table 6. The degree of conversion, X_{CaO}, as a function of time is plotted in Fig. 5 at different temperatures. It can be seen that conversion increased sharply in the first 10 minutes. But after 10 minutes, it seems the mechanism of reaction starts to change and the conversion-time curve changes more slowly. The effect of temperature on the reaction can be shown in this figure as well. For about the first 10 minutes simultaneous chemical reaction and diffusion control the rate of reaction. After 10 minutes as the reaction proceeds, the formation of a thin layer of $CaCO_3$ influences a progressive change in the reaction rate towards the diffusion control regime governed by CO_2 diffusion through the $CaCO_3$ layer. In the first part of the curve the best fit of modeling results with experimental data can be achieved by justifying the frequency factor of kinetic relationship and diffusion coefficient of the CO_2 in product layer. But in the second stage of reaction, the diffusion of CO_2 through the product layer is the only controlling parameter.

In the regime where both kinetic and diffusion control the reaction rate, the diffusion coefficients were justified at different temperatures as reported in Table 5. The Arrhenius plot can be considered to give a good estimate for the activation energy for product layer diffusion in this regime. Fig. 6 shows the Arrhenius plot as Ln D_{AG} versus 1/T yielding a value of 210 kJ mol^{-1} for the activation energy. This value is within the scale of that reported by Bhatia and Perlmutter [3], at 179 kJ mol^{-1}.

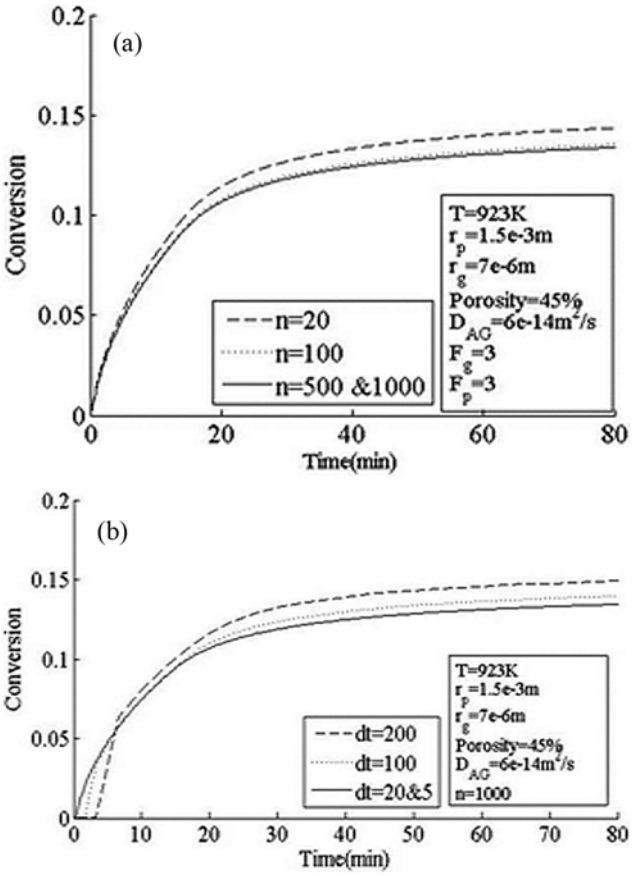

Fig. 7. Effect of different computational parameters of program, (a) total numbers of grids in the pellet, (b) time step.

The dependence of program results on the total number of grids in the pellet, n, and the value of time steps, dt, are shown in Figs. 7(a) and 7(b). At the number of grids higher than 100, the conversion curve is independent of the number of grids. Also, if the time step is less than 20 sec, the conversion curve is unaffected.

Fig. 8 shows the CO_2 concentration profile inside the pellet at 650 °C for varying porosity. At a high porosity of 45% (Fig. 8(a)) the variation of concentration in the pellet is small, while decreasing the porosity to 30% (Fig. 8(b)) results in a greater variation of CO_2 concentration inside the pellet.

The porosity inside the pellet is subject to change with time because of changing grain radius. Variation in molar density of CaO and $CaCO_3$ can cause decrease in porosity. Figs. 9(a) and 9(b) show the porosity and grain radius variation in the pellet of CaO at 650 °C.

As can be seen in Fig. 9(a) the pellet porosity varies from an initial value of 45% to 39% uniformly for all nodes inside the pellet consistent with the CO_2 concentration results inside pellet as shown in Fig. 8(a). The grain radius is increased from 7 μm to 7.3 μm as the reaction proceeds as shown in Fig. 9(b).

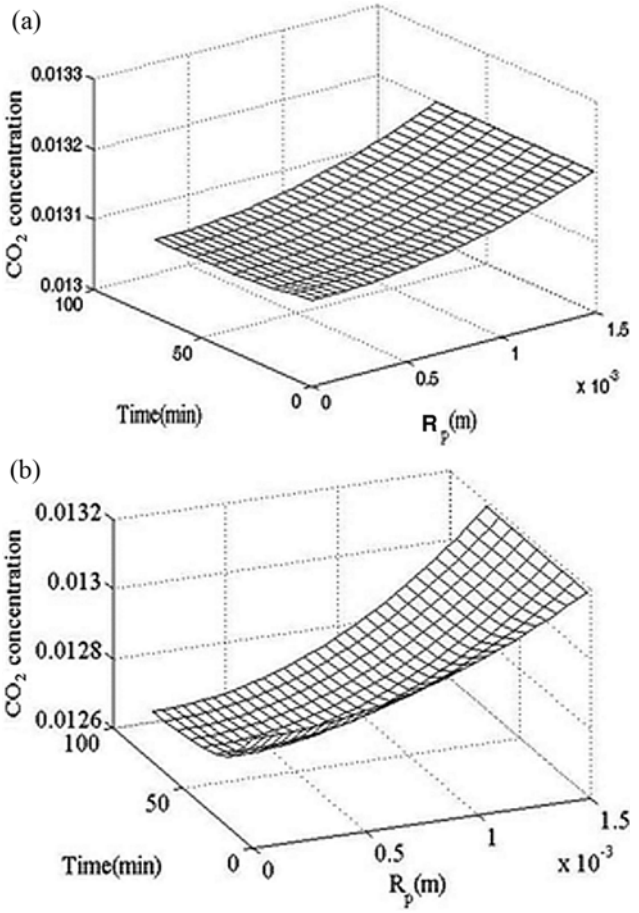

Fig. 8. CO_2 concentration profile inside the pellet at 650 °C, (a) ε= 45%, (b) ε=30%.

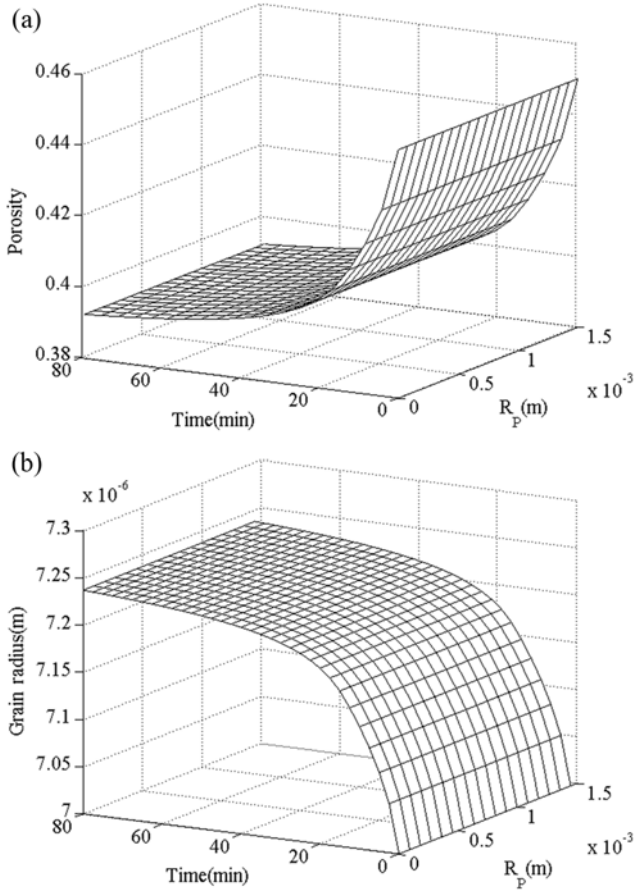

Fig. 9. Variation of (a) porosity and (b) grain radius, in the CaO pellet.

The radial position of reaction front, r_c, as a function of time is shown in Fig. 10. As can be seen the reaction front varies from 7 μm equal to initial grain radius to about 6.9 μm as the reaction reaches to the end. In other words, a product layer of about 0.1 μm thickness can decrease the rate of the reaction while shifting the controlling step of reaction to diffusion control regime.

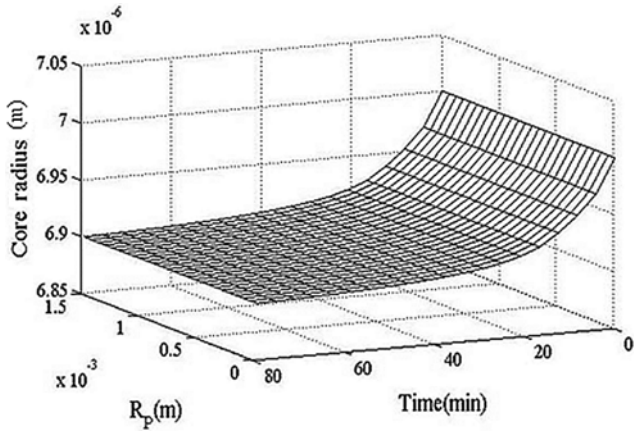

Fig. 10. Variation of r_c as a function of time in the pellet.

SCOPE OF THE MODEL PREDICTIONS

A comparison between modeling results and experimental data shows the limitations of using the model. As it is seen from the Figs. 3-5, the mathematical modeling predicts acceptable results at higher temperatures rather than at lower temperatures. Higher temperature in a gas-solid reaction results in higher kinetic rates in comparison with diffusion rates for the gas through the product layer. Under this condition with increasing the temperature, the controlling stage of the reaction will shift from a kinetic controlling stage to a mixed kinetic and diffusion controlling step or a diffusion alone controlling step. By considering the diffusion phenomenon in the early stages of the reaction in the present work, the model generates better predictions.

SENSITIVITY ANALYSIS STUDIES

A sensitivity analysis study was carried out on the reaction of a pellet at 923 K with the aim of investigating the role of different parameters on the conversion and for finding the significant parameters to obtain a higher conversion.

1. Porosity Effect

The pellet porosity is an important parameter that can change the final conversion of the pellet. Fig. 11 shows conversion curves at different pellet porosities. As expected the more porous pellets result in higher conversion. Higher porosity leads to greater unifor-

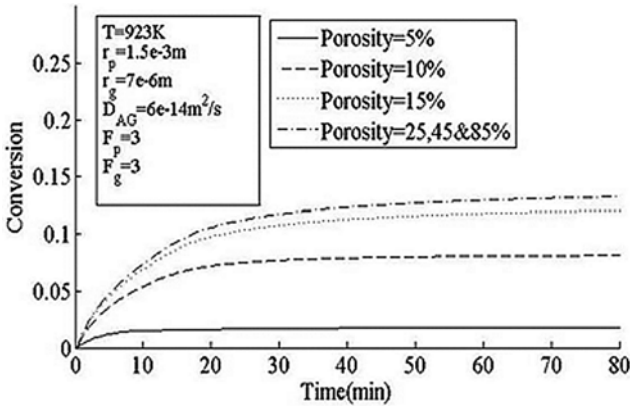

Fig. 11. Effect of pellet porosity on the conversion.

mity of the gaseous reactant concentration inside the pellets, resulting in higher conversion until a value of 25% porosity. The conversion curve does not change at porosities greater than 25% at which the gas reactant concentrations can be assumed to reach a constant uniform value through the pellet. Also, the effect of porosity on conversion decreases as the porosity values become higher.

2. Pellet Size Effect

The pellet radius can also affect the conversion curve. Choosing higher pellet radius causes lower conversion. In this case the diffusion of gaseous reactant inside the pellet plays a significant role, and in fact a higher radius can result in increasing diffusion distance for gas, leading to lower conversion. Porosity will play a part as well. Fig. 12 shows the effect of pellet radius on conversion at different porosities at a selected temperature of 650 °C. As it can be seen at

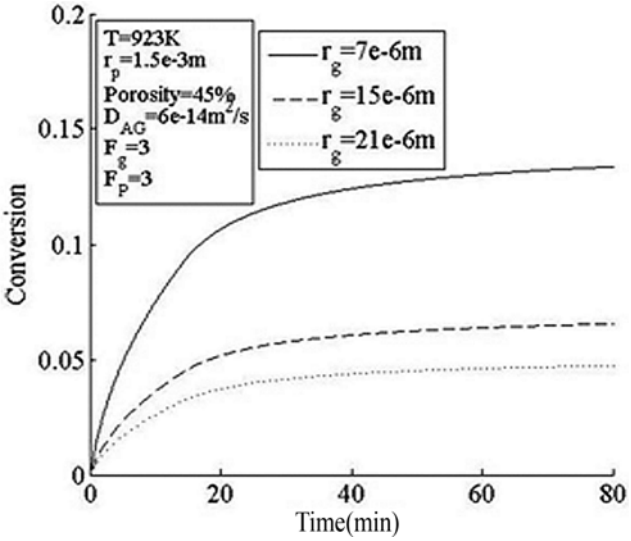

Fig. 13. Effect of grain size on the conversion curve.

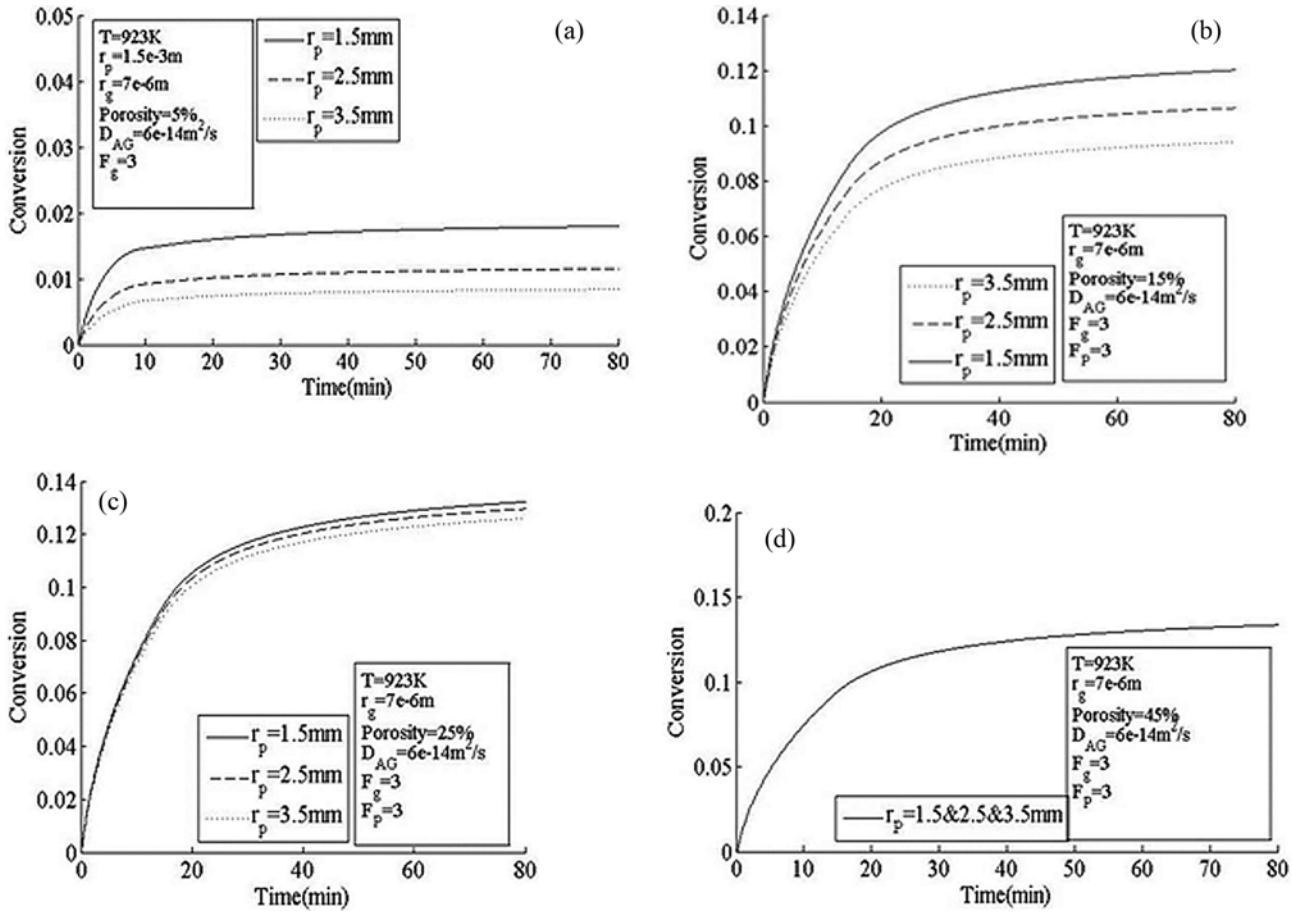

Fig. 12. Effect of pellet radius on conversion, (a) 5% porosity, (b) 15% porosity, (c) 25% porosity, and (d) 45% porosity.

higher porosities >25%, the conversion curves are closer to each other and produce overlapping curves at 45% porosity. When the porosity value is increased to 25% the diffusion of gas inside the pellet is not an important factor as the gas concentration is constant and uniform throughout the pellet.

3. Grain Size Effect

The grain size is the other parameter that can change the conversion curve. Fig. 13 shows the effect of grain radius on conversion at 650 ºC. Reducing the grain size from 15 μm to 7 μm has the effect of increasing the conversion nearly by a factor of two, arising from increasing surface area for the reaction.

4. Grain and Pellet Geometry Effects

Effect of different grain and pellet geometrical shapes on the degree of conversion is reported in Fig. 14 and Fig. 15. The spherical grains show a higher degree of conversion in comparison with other geometries because of higher reaction area availability in spherical grain geometry than other geometries as shown in Fig. 14(a). As shown in Fig. 14(b), there is no change in conversion curve in the different pellet geometries at 45% porosity and a pellet radius of 1.5 mm. Both the gas diffusion in the pellet and pellet geometry do not have any further significance.

Fig. 15 shows the effect of pellet geometries on conversion for the same pellet but at different porosities of 5%, 15% and 25%. In this case different curves were produced that show higher final conversion for spherical pellets. The reason for this increased conversion in the case of the spherical pellet geometry can be related to achieving a uniform constant gas concentration because of reducing the effect of the gas diffusion in spherical geometry in comparison with other geometries.

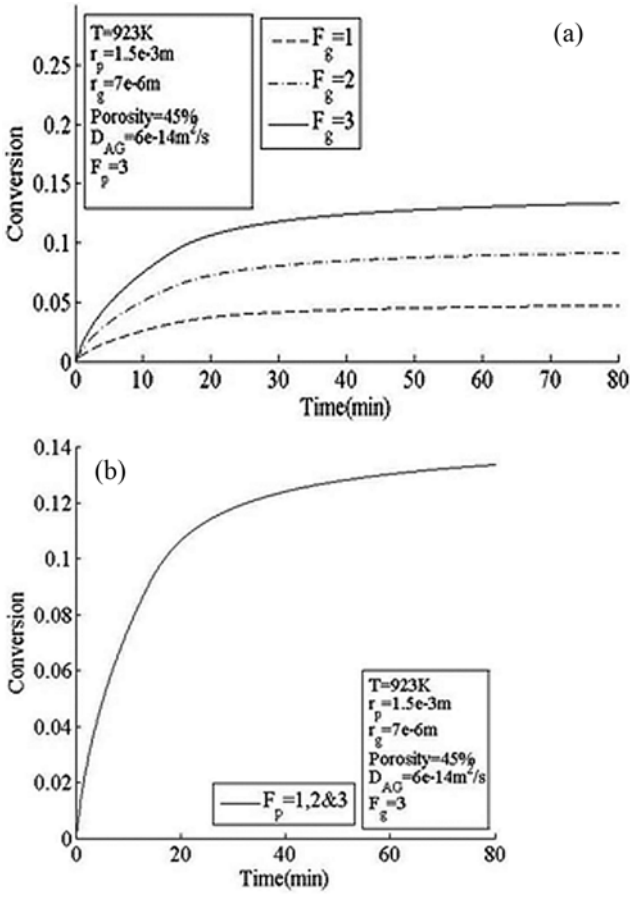

Fig. 14. Effect of (a) grain geometries, and (b) pellet geometries on the conversion curve.

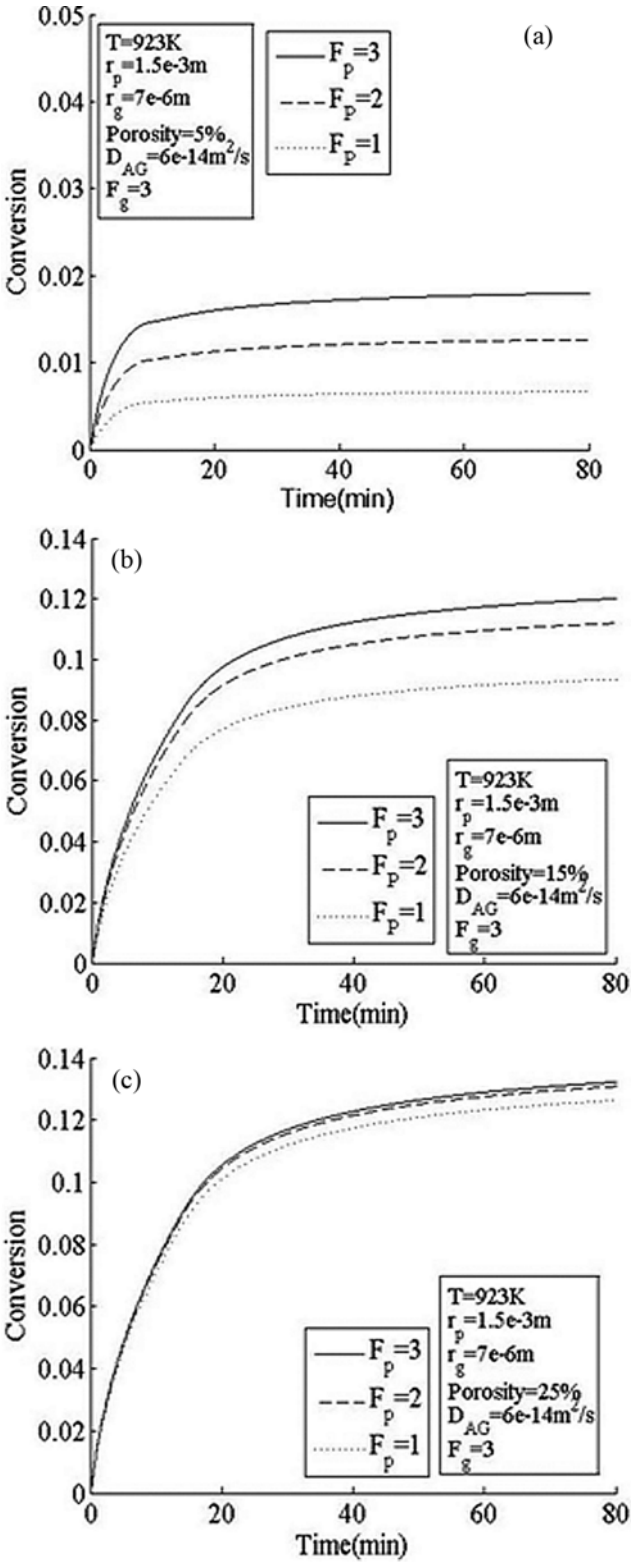

Fig. 15. Effect of pellet geometries on conversion, (a) 5% porosity, (b) 15% porosity and (c) 25% porosity.

SUMMARY

The carbonation reaction of CaO with CO_2 was mathematically modeled through two stages of rate controlling regimes. In the first stage, the rate of CaO carbonation was controlled by the reaction kinetics and diffusion through the product layer around grains, simultaneously, and in the second stage, after the layer of solid product was formed, the rate of CaO carbonation was controlled by gaseous reactant diffusion alone through the solid product around the grains. The blockage of microscopic pores during the reaction due to solid product formation decreases the rate of CaO carbonation and changes the rate controlling regime from the combined chemical reaction and diffusion controlling regime to pure diffusion control regime.

The grain model was developed and used to study the carbonation reaction with justifying the frequency factor of reaction rate equation and reactant diffusion coefficient, D_{AG}, to get the best fit at different temperature range from 400 to 750 °C with respect to experimental data taken from the literature. The present model predicts acceptable results in the domain that the diffusion of gas through the product layer can be significant and plays a major role in controlling stage of the reaction.

The model was also used to study the sensitivity analysis of the carbonation reaction. The porosity is seen to be the most sensitive parameter for affecting the conversion behavior.

NOMENCLATURE

A, B : constants in Eq. (12)
C : concentration [kmol m^{-3}]
$C_{CO2,i,f}$: final CO_2 concentration at reaction front [kmol m^{-3}]
$CaCO_3$: calcium carbonate
CaO : calcium oxide
CO_2 : carbon dioxide
D : diffusion coefficient [m^2 s^{-1}]
D_e : effective diffusivity [m^2 s^{-1}]
D_K : Knudsen diffusivity [m^2 s^{-1}]
D_M molecular diffusivity [m^2 s^{-1}]
E_a : activation energy [J $kmol^{-1}$]
F_p, F_g : pellet and grain shape factors, (=1, 2 and 3 for flat, cylindrical and spherical geometries, respectively)
f_G : rate of surface reaction [kmol m^{-2} s^{-1}]
k : reaction rate constant
k_c : convective mass transfer coefficient [m s^{-1}]
k_0 : a constant in Eq. (24)
k′ : frequency factor [m s^{-1}]
M : molecular weight [kg $kmol^{-1}$]
n : a constant in Eq. (12)
n_d : number of solid grains per unit volume of porous solid
R : ideal gas constant [J $kmol^{-1}$ K^{-1}]
R_p : radial coordinate in the pellet [m]
r_c : radial position of the reaction front inside pellet [m]
r_0 : initial radius of grains [m]
r_g : grain radius [m]
r_p : pellet radius
T : temperature [K]
t : time [s]
$t_{f,1}$: final time in the first stage
X : overall conversion of pellet
x : conversion of grains
z : radial coordinate in the pellet [m]

Greek Letters

ε : porosity
ρ : density [kg m^{-3}]
τ : tortuosity of pellet

Subscripts

0 : initial value
b : bulk
i : interface between product layer and the solid reactant
p : product layer
s : on the pellet surface

REFERENCES

1. S. Eloneva, *Mineral carbonation process modeling and carbonate product stability*, Helsinki University of Technology (2004).
2. T. Koljonen, H. Siikavirta and R. Zevenhoven, CO_2 Capture and Storage and Utilization In Finalnd, Valtion teknillinen tutkimuskeskus, Project Report PRO4/T7504/02, 95 (2002).
3. S. K. Bhatia and D. D. Perlmutter, *AIChE J.*, **29**, 1, 79 (1983).
4. A. J. Dedman and A. J. Owen, *Trans. Soc.*, **58**, 2027 (1982).
5. W. G. Oakeson and I. B. Culter, *J. Am. Cream. Soc.*, **62**, 11&556 (1979).
6. H. Gupta and L. S. Fan, *Ind. Eng. Chem.*, **41**, 4035 (2002).
7. D. K. Lee, I. H. Baek and W. L. Yoon, *Chem. Eng. Sci.*, **59**, 931 (2004).
8. D. K. Lee, *Chem. Eng. J.*, **100**, 71 (2004).
9. V. Nikulshina, M. E. G´alvez and A. Steinfeld, *Chem. Eng. J.*, **129**, 75 (2007).
10. B. R. Stanmore and P. Gilot, *Fuel Process. Technol.*, **86**, 1707 (2005).
11. B. Khoshandam, R. V. Kumar and E. Jamshidi, *Trans. Inst. Min. Metall. C*, **114**, C10 (2005).
12. J. Szekely, J. W. Evans and H. Y. Sohn, *Gas-solid reactions*, Academic Press, New York (1976).
13. O. Levenspiel, *Chemical reaction engineering*, Wiley, New York (1965).
14. N. Wakao and J. M. Smith, *Chem. Eng. Sci.*, **17**, 825 (1962).
15. C. N. Satterfield, *Mass transfer in heterogeneous catalysis*, MIT Press, Cambridge, MA (1970).
16. E. A. Mason, A. P. Malinauskas and R. B. Evans, *J. Chem. Phys.*, **46** (1967).